THIS MONTH IN
JNM

PET and circulating tumor cells: Yu and Cristofanilli focus on recent advances in molecular characterization of tumor cells in peripheral blood in advanced cancers and associated implications for monitoring of targeted therapies. . . . . ***Page 1501***

Scintigraphy for pulmonary embolism: Sostman and Pistolesi offer perspective on the reliability and clinical relevance of this technique and preview a related article in this issue of *JNM*. . . . . ***Page 1505***

Ternary interpretation of V/Q scans: Glaser and colleagues describe a new and simplified interpretive strategy to improve on probability-based assessments in scintigraphic studies of pulmonary embolism. . . . . ***Page 1508***

PET/CT V/Q imaging with ^{68}Ga: Hofman and colleagues explore the feasibility of using PET/CT to perform ventilation–perfusion assessment of lung function and compare its diagnostic effectiveness with that of conventional V/Q scintigraphy in patients with suspected pulmonary embolism. . . . . ***Page 1513***

Virtual ^{18}F-FDG PET/CT bronchoscopy: Herbrik and colleagues determine the diagnostic accuracy of fly-through 3-dimensional ^{18}F-FDG PET/CT bronchoscopy for detection of regional lymph node metastases in non–small cell lung cancer. . . . . ***Page 1520***

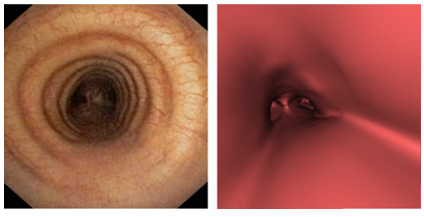

PET/CT for initial breast cancer staging: Groheux and colleagues evaluate the role of ^{18}F-FDG PET/CT in patients with stage IIA, IIB, or IIIA breast cancer. . . . . ***Page 1526***

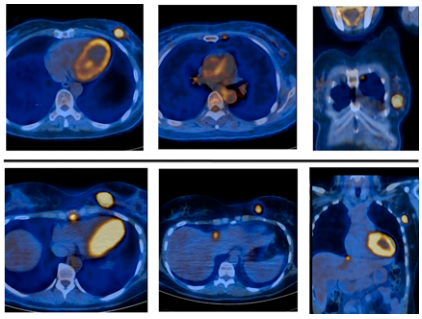

PET and outcomes in rhabdomyosarcoma: Baum and colleagues investigate the role of ^{18}F-FDG PET or PET/CT in prediction of outcomes and in refinements in risk-adapted therapy in children and young adults affected by this soft-tissue sarcoma. . . . . ***Page 1535***

PET and estrogen receptors: Kurland and colleagues use ^{18}F-fluoroestradiol PET to quantify within-patient and between-patient heterogeneity of estrogen receptor expression in breast cancer lesions. . . . . ***Page 1541***

Tumor delineation evaluation: Cheebsumon and colleagues assess test–retest variability in automatic and semiautomatic tumor delineation methods, including the effects of image characteristics and resulting implications for both target volume planning and monitoring of therapy response. . . . . ***Page 1550***

SPECT and arrhythmic risk: Paul and colleagues use ^{123}I-MIBG SPECT to investigate the role of adrenergic dysfunction in patients with arrhythmogenic right ventricular cardiomyopathy and correlate these findings with genotypic data. . . . ***Page 1559***

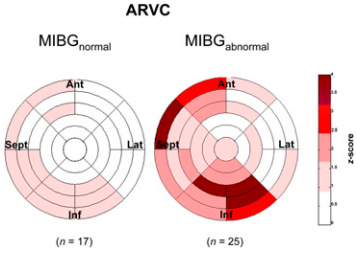

Measuring hepatic galactose metabolism: Sørensen and colleagues quantify hepatic galactose elimination in healthy humans using ^{18}F-FDGal PET for assessment of regional liver function. . . . . ***Page 1566***

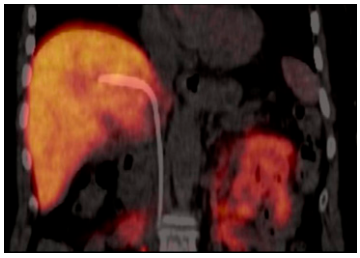

Molecular imaging and EGFR-TKI: Meng and colleagues look at information provided by an ^{11}C-labeled PET biomarker of epidermal growth factor receptor in patients with non–small cell lung cancer treated with EGFR tyrosine kinase inhibitor erlotinib. . . . . ***Page 1573***

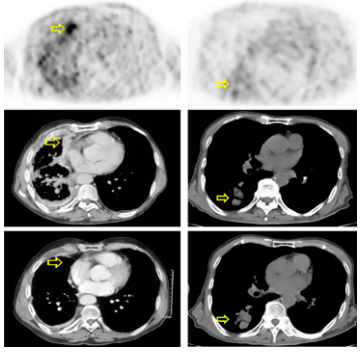

PET/CT lymphoscintigraphy: Heuveling and colleagues describe the development and initial evaluation of a nanocolloidal albumin–based tracer designed for sentinel node detection with high-resolution PET. . . . . ***Page 1580***

Tumor recurrence imaging: Heiss and colleagues provide an educational overview of multimodality assessment of brain tumors and tumor recurrence, with a focus on PET, MRI, and soon-to-be-widely available

integrated whole-body PET/MRI systems. . . . . *Page 1585*

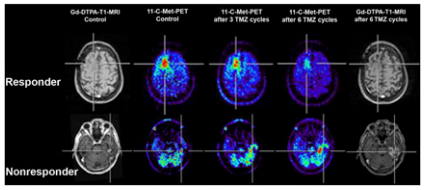

mAb imaging of prostate cancer: van Rij and colleagues examine the characteristics of a humanized IgG1 monoclonal antibody directed against the epithelial glycoprotein-1 and assess the potential for immuno-PET and immuno-SPECT imaging in mice with human prostate cancer xenografts. . . . . *Page 1601*

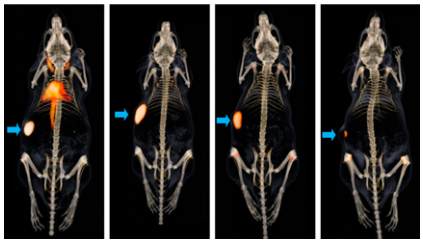

^{89}Zr-7E11 immuno-PET of PSMA: Ruggiero and colleagues report on preparation and in vivo evaluation of a novel radiolabeled monoclonal antibody construct for targeted imaging of prostate-specific membrane antigen, a prototypical cell surface marker overexpressed in prostate cancer. . . . . *Page 1608*

Tracer accumulation and BAT heat: Carter and colleagues explore in mice the relationship between stimulation of ^{18}F-FDG accumulation in brown adipose tissue by 3 stressors and heat production measured in vivo by thermal imaging. . . . *Page 1616*

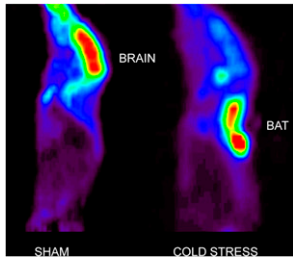

Coregistration of multimodality images: Axente and colleagues describe development and evaluation of deformable coregistration of autoradiography and microscopy images from sequential sections and discuss the utility of this approach in histopathologic validation of PET tracers. . . . . *Page 1621*

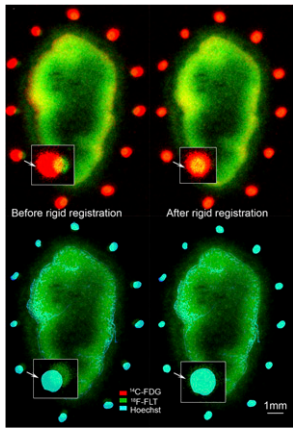

Targeted radiotherapy with scVEGF/^{177}Lu: Blankenberg and colleagues investigate whether high levels of vascular endothelial growth factor receptor in tumor vasculature can be leveraged for intracellular delivery of therapeutically significant doses of a novel radiopharmaceutical in orthotopic breast cancer models. . . . . *Page 1630*

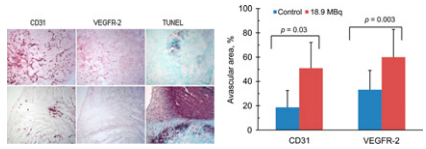

PET of NOP receptors in monkeys: Kimura and colleagues assess the biodistribution of an ^{11}C-labeled radioligand for a nociceptin/orphanin FQ peptide receptor and its ability to quantify these receptors in monkey brain. . . . . *Page 1638*

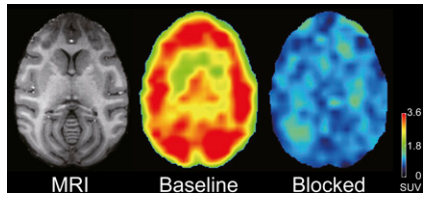

NEMA NU 4 in small-animal SPECT: Harteveld and colleagues determine for a small-animal multipinhole SPECT scanner the image quality parameters associated with the National Electrical Manufacturers Association NU4 phantom. . . . *Page 1646*

PET in prostate cancer models: Kukuk and colleagues evaluate PET with various tracers in 2 hormone-independent prostate cancer xenograft mouse models and compare the results with immunohistochemistry and surgical outcomes. . . . *Page 1654*

ON THE COVER

A pilot study has shown V/Q PET/CT to have advantages over conventional V/Q imaging, including superior image quality and the potential for better regional quantitation of lung function. In the patient shown here, with severe chronic obstructive airway disease, PET/CT enabled exclusion of PE with high confidence compared with SPECT/CT, which was deemed nondiagnostic.

See page 1516.